Short Report

Journal of the Brazilian Chemical Society

https://dx.doi.org/10.21577/0103-5053.20230122

J. Braz. Chem. Soc. **2024**, *35*, 2, e-20230122, 1-7

Gold Nanoparticles Supported on Triazole-Functionalized Biochar as Nanocatalyst for Hydrogen Evolution from Aqueous Solution

Renata P. Lopes, [a,b] ***Qiuxia Zhao,*** [b] ***Sergio Moya,*** [c] ***Marta M. Moro*** [c] ***and Didier Astruc****[b]

[a]*Departamento de Química, Universidade Federal de Viçosa, 36570-900 Viçosa-MG, Brazil*

[b]*Université de Bordeaux, ISM, UMR CNRS 5255, Talence 33405 Cedex, France*

[c]*Soft Matter Nanotechnology Lab, CIC biomaGUNE, Paseo Miramón 182, 20014 Donostia-San Sebastián, Gipuzkoa, Spain*

Biochar is a material of great ecological interest obtained from the carbonization of biomass. Its structure is composed of graphene-like aggregates, and it contains useful functional groups such as carboxyl. Using these groups, biochar functionalization with triazole groups that improve support characteristics has been achieved to anchor and stabilize catalytically active gold nanoparticles (Au NPs). The Au NPs obtained were homogeneously distributed under biochar, with a size of 7.7 ± 3.5 nm. The efficiency of the nanomaterial was shown in nanogold-catalyzed hydrogen evolution from an aqueous solution containing $B_2(OH)_4$, with a maximum hydrogen generation of 715 $mL_{H_2} g_{cat}^{-1} min^{-1}$ under optimized conditions (0.070 mmol of Au NPs and 0.300 mol L^{-1} of NaOH). This nanomaterial showed excellent efficiency in four successive catalytic cycles.

Keywords: Au NPs, biochar, H_2 evolution, catalysis

Introduction

Hydrogen has highlights as a clean and sustainable energy source, as it has a high energy density *per* unit mass and generates water as a by-product of combustion.[1] Hydrogen can be produced from different processes, including fossil sources such as petroleum, from biomass[2] and water electrolysis.[3,4] However, H_2 storage is problematic because it is in gaseous form under environmental conditions, resulting in low energy *per* volume (12.7 MJ m^{-3} *versus* 40 MJ m^{-3} for CH_4),[5] in addition, transport is dangerous, hydrogen being highly explosive. Thus, chemical hydrogen storage has attracted intense attention during the last two decades. This technology is based on the chemical bond between a heteroatom, preferably light, and atomic hydrogen, whose breakage is responsible for the formation of H_2 through intra/intermolecular reactions.[5] Boron-based chemical hydrides, such as NH_3BH_3,[6-9] $NaBH_4$,[10] $B_2(OH)_4$,[11-13] among others are attractive candidates as hydrogen sources for mobile and stationary applications at ambient or moderate temperature.[14] The hydrolysis of tetrahydroxydiboron, $B_2(OH)_4$, occurs according to the equation 1.

$$B_2(OH)_4 + 2\ H_2O \rightarrow 2\ B(OH)_3 + H_2\uparrow \quad (1)$$

Various supported late transition-metal nanocatalysts have been employed in the production of hydrogen using aqueous solutions of boron-based chemical hydrides[15-18] including Pd, Pt and Ag nanoparticles supported on magnetic biochar.[10] However, gold nanoparticles (Au NPs) have high chemical stability and improved kinetics under aerobic conditions.[6] Besides, Au NPs present assembly of multiple types involving materials science, with behavior of the individual particles, such as size-related electronic, magnetic and optical properties (quantum size effect).[19] Such properties allow catalytic use of Au NPs in several areas, in particular in the evolution of hydrogen from inorganic hydrides.[6,13] However, nanomaterials have a natural tendency to agglomerate, decreasing catalytic efficiency. To avoid this phenomenon, these nanomaterials can be anchored onto support materials that, in addition to improved dispersion, can also be used in a heterogeneous configuration, allowing reuse. Biochar of various types is a strong candidate for use as a support.[18]

Biochar is a product of the biomass carbonization of high ecological interest.[18] Its structure consists of graphene-like aggregations, containing carboxylic, carbonyl and phenolic groups.[18] To improve the characteristics of biochar, various kinds of functionalization have been described in

*e-mail: renata.plopes@ufv.br; didier.astruc@u-bordeaux.fr
Editor handled this article: Célia M. Ronconi (Associate)

the literature. Bamdad *et al.*[20] modified biochar by two different methods: (*i*) nitration, followed by reduction, and (*ii*) condensation of aminopropyl triethoxysilane on the surface. Sajjadi *et al.*[21] produced a biochar physically modified by low frequency ultrasound irradiation, treatment by H_3PO_4 and functionalization by urea. Xiong *et al.*[22] synthesized sulfonated wood waste-derived biochar as catalysts for the production of value-added chemicals from carbohydrates.

Modified biochars for evolution of hydrogen from hydrides are described in the literature. Akti[23] synthesized pistachio shell-derived biochar supported cobalt catalyst (Co-PDA@BC) and applied it to the hydrogen evolution from $NaBH_4$. According to the author, the maximum hydrogen generation rate and activation energy were 25 mL min^{-1} g_{cat}^{-1} and 31.3 kJ mol^{-1}, respectively. Li *et al.*[24] anchored $NiCoO_2$ nanoparticles on biochar from waste coffee. The authors evaluated the catalytic performance of the catalyst in the hydrogen generation from NH_3BH_3 hydrolysis, which produced 4 mmol of H_2 in less than 15 min of reaction. Saka[25] produced a metal-free carbon from microalgae (*Spirulina plasentis*) that was doped with sulfur and phosphorus which was used as catalyst for $NaBH_4$ methanolysis for hydrogen evolution. The author obtained a hydrogen generation rate (HGR) of 18,571 mL min^{-1} g^{-1}. In another work, Saka[26] produced a carbon derived from the microalgae *Chlorella vulgaris*, also doped with sulfur and phosphorus, which was used as a catalyst for $NaBH_4$ methanolysis. In this work, the HGR was 13,000 mL min^{-1} g^{-1}. Another work by Saka[27] consisted of the synthesis of carbon-free metal doped with oxygen (O) and nitrogen (N) from the microalgae *Spirulina platensis*. In this work, the author obtained 10,105 mL min^{-1} g^{-1}. However, $NaBH_4$ methanolysis reaction that takes place in a non-green solvent.

Several ligands can be used to stabilize Au NPs such as sulfur ligands (thiolate ligands), cetyltrimethylammonium bromide (CTAB), nitrogen donors (imidazoles, pyridines). Regarding such ligands, the 1,2,3-triazole ring is an amphoteric π-electron-rich aromatic, biocompatible and stable toward both oxidizing and reducing agents.[28] However, as far as know, there is no work using Au NPs anchored in biochar, especially functionalized with a triazole group, for the hydrolysis of $B_2(OH)_4$.

As described above, Au NPs have excellent catalytic activities in diverse applications.[19,29-33] Various supports have been used to prevent the agglomeration and coalescence of Au NPs and increase the activities of these nanocatalysts. Nitrogen heterocycles such as triazole have been employed as stabilizing agents.[34] Therefore, this work aimed to functionalize biochar with thiazole groups followed by chemical deposition of gold nanoparticles and apply them in the production of hydrogen using aqueous solutions of $B_2(OH)_4$.

Experimental

Chemicals and reagents

Sodium hydroxide (CAS 1310-73-2) was obtained from Fisher (Hampton, Nova Hampshire, USA). Sodium borohydride (CAS 16940-66-2) and trihydrate chloroauric acid (CAS 16961-25-4) were obtained from Alfa Aesar (Haverhill, Massachusetts, USA). Acetone, benzyl chloride (CAS 100-44-7), thionyl chloride (CAS 7719-09-7), tetrahydrofuran (CAS 109-99-9), sodium azide (CAS 26628-22-8), potassium carbonate (CAS 584-08-7), copper(II) sulfate pentahydrate (CAS 7758-99-8), tetrahydroxydiboron (CAS 13675-18-8) and sodium ascorbate (CAS 134-03-0) were purchased from Sigma-Aldrich (Saint Louis, Missouri, USA). Propargylamine (CAS 2450-71-7) was purchased from Acros (Geel, Antwerp Belgium). All reagents were analytical grade used without any purification steps. Aqueous solutions were prepared with water type 1 obtained by Milli-Q system (Millipore, Bedford, MA, USA).

Preparation of biochar

Arabica coffee straw was collected in Espírito Santo-Brazil, washed with distilled water, dried to 80 ºC for 48 h and ground in a knife mill. The biomass was added in a hollow cylinder with a lid containing a small hole for the exit of generated gases. This condition limits the oxygen ingress. The system was placed in a muffle previously heated to 600 °C, staying for 4 h. Finally, biochar was sieved to form particles of 20-200 mesh.

Benzylazide synthesis

Two milliliters (2 mL) of benzyl chloride, 1.40 g of sodium azide and 40 mL of acetone were added in a flask. The system was kept under reflux at 80 °C under constant agitation during 24 h. After that, the system was reserved for a later step.

Biochar (BC)-triazole synthesis

The material was synthesized according to Pereira *et al.*[35] Firstly, the carboxyl group present in the biochar was converted into an acyl group, as shown in the equation 2 (Figure 1). For this, 0.50 g of biochar and 30 mL of $SOCl_2$ were added to a flask.

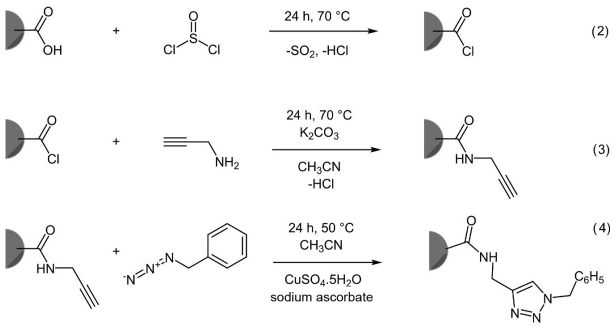

Figure 1. Scheme for the synthesis of triazole-functionalized biochar (adapted from reference 35).

The system was kept under stirring for 24 h under reflux at 70 °C. Then, the material was centrifuged (5 min at 5000 rpm) and subjected to three washing steps with tetrahydrofuran. The material was transferred to a flask under which 25 mL of acetonitrile, 3 mmol of K_2CO_3 and 3 mmol of propargylamine were added, according to equation 3, obtaining biochar with terminal alkyne. The material was centrifugated (5 min at 5000 rpm) and subjected to three washing steps with type 1 water, followed by washing with acetone. The material was transferred to the system containing benzylazide, in which 0.34 mmol $CuSO_4 \cdot 5H_2O$ and 3.4 mmol sodium ascorbate were added (equation 4).[36,37] The system was kept under constant agitation at 50 °C for 24 h, forming the triazole-functionalized biochar (BC-triazole).[35]

Au-BC-triazole synthesis

The synthesis of Au NPs was performed according to Zhao *et al.*[13] 500 mg BC-triazole was added in a flask, to which 0.19 mmol of $HAuCl_4 \cdot 3H_2O$ dissolved in 5 mL of water were added. The system was kept under stirring for 30 min. After that, 1.00 mmol of sodium borohydride, $NaBH_4$, dissolved in 1.00 mL of water, was added to the system that was kept under stirring for another 10 min. The system was centrifuged and subjected to three washing steps with water type 1 and dried under vacuum.

The material was characterized by infrared spectroscopy using Bruker VERTEX 70 instrument (Billerica, USA) using the attenuated total reflection (ATR) method in the range of 350-4000 cm^{-1}. The material was also analyzed by transmission electron microscopy (TEM), TEM JEOL JEM 1400, 120 kV (Akishima, Tokyo, Japan). The Au NPs size was determined for forty nanoparticles (n = 40) using ImageJ.[38] X-ray photoelectron spectroscopy (XPS) was used to evaluate the species present in the material. It was used a system: SPECS SAGE HR, X-ray source: Mg Kα non-monochromatic, operated at 12.5 kV and 250 W. Take-off angle 90°, at ca. 10^{-8} Torr. Pass energy for survey spectra 30 eV, 15 eV for narrow scans.

H_2 evolution from $B_2(OH)_4$

The H_2 evolution from $B_2(OH)_4$ was performed according to Zhao *et al.*[13] The amount of Au-BC-triazole was transferred to a 50 mL Schlenk flask under which 5 mL of 0.600 mol L^{-1} NaOH was added. The system was properly sealed and coupled via the gas outlet to a water-filled gas burette. 90 mg (1 mmol) of $B_2(OH)_4$ was dissolved in 5 mL of water and inserted into the bottle using a syringe. The system was kept under constant agitation at a controlled temperature of 30 °C. A quantitative conversion of $B_2(OH)_4$ produced 1.0 equivalent of H_2, and occupied ca. 22.4 mL at atmospheric pressure. Prior to the reactions, the volumes were measured at atmospheric pressure and corrected for water vapor pressure at room temperature.

Reuse assays were conducted. For this, after the first cycle, the material was subjected to three stages of washing with water type 1 and reintroduced into the system in the conditions previously described.

Results and Discussion

First, Au NPs decorated in biochar without functionalization, i.e., without triazole groups, were used in the reaction of hydrogen production from $B_2(OH)_4$; however, the yield was very low. The specific surface area of biochar before functionalization was determined as in a previous work (1.242 m^2 g^{-1}).[39] Although the surface area is low, this material has functional groups that can be functionally linked to improve catalytic efficiency. Since biochar has carboxyl groups in its structure,[18] a strategy for biochar functionalization with the 1,3-triazole group, a smooth stabilizer for Au NPs, was considered.[34] This strategy consisted of the introduction of a terminal alkyne, followed by a Cu^I-catalyzed azide-alkyne cycloaddition (CuAAC) "click" reaction[36,37] with benzylazide. First, the introduction of the terminal alkyne was performed, as shown in equations 2 and 3. As can be seen in Figure 2, the introduction of this functional group was successful. It is possible to observe a band in the 2908 cm^{-1} region attributed to the C–H binding, confirmed by the band in 2852 cm^{-1}. A band is observed in 1698 and 1463 cm^{-1} and attributed to the presence of amide. After the CuAAC "click" reaction with benzylazide, the material did not show the bands related to the terminal alkyne. However, it is possible to observe the presence of a peak referring to the amide at 1635 cm^{-1}.

After functionalization, Au NPs were deposited by a chemical reduction method with sodium borohydride. The

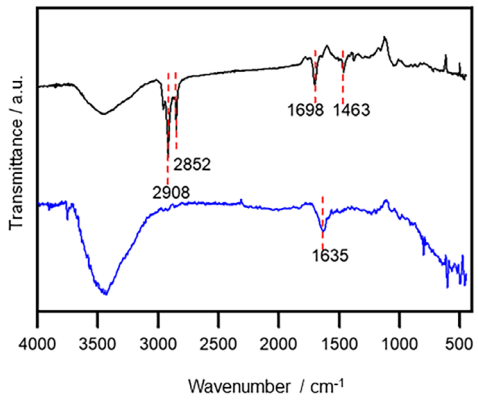

Figure 2. FTIR (ATR) spectra of (—) BC-$CONH_2CCH$ and (—) BC-1,3-triazole.

material was analyzed by TEM, Figure 3. The Au NPs are homogeneously distributed on the surface of the biochar, presenting a *quasi*-spherical format of size 7.7 ± 3.5 nm. The histogram is shown in Figure 4. $NaBH_4$ plays a key role in determining the AuNP size.[9] The functionalization allowed homogeneous distribution of Au NPs, avoiding their coalescence and agglomeration. The catalytic efficiency is very dependent on the size and dispersion of the nanoparticles.

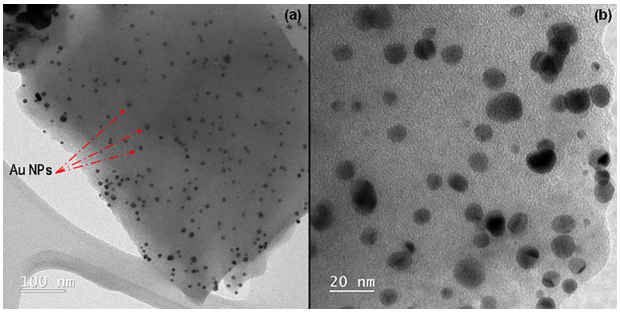

Figure 3. TEM images of Au-BC-triazole. Au NPs 7.7 ± 3.5 nm (n = 40).

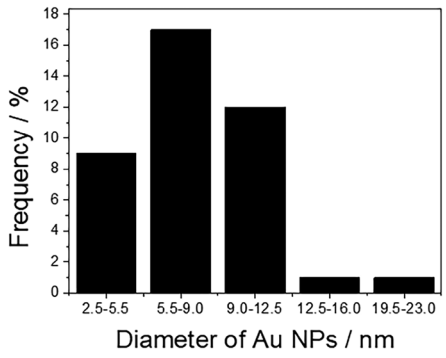

Figure 4. Histogram of Au NPs. Size: 7.7 ± 3.5 nm (n = 40).

The oxidation state of the elements present in the material was determined by XPS. Binding energies (BE) of 84.5 and 88.3 eV are observed for levels $4f_{7/2}$ and $4f_{5/2}$, respectively, and can be attributed to Au^0 (Figure 5a). Similar results were observed by Zhao *et al.*,[13] who applied the material in the evolution of hydrogen from $B_2(OH)_4$. BE of 284.8, 286.4 and 288.4 eV are attributed to C–C, C=O and O–C=O, respectively (Figure 5b). BE of 532.1 and 532.8 eV are attributed to carbon-bound oxygen in the forms of C=O and C–O–H, respectively (Figure 5c). Finally, 400.6 eV BE is attributed to carbon-bound nitrogen (Figure 5d). These results of C, O and N bonds are in agreement with those observed in FTIR and confirm the formation of the triazole group.

The material was applied in the hydrogen evolution reaction, under different concentrations of sodium hydroxide, and the results are shown in Figure 6. According to Wang *et al.*,[15] the presence of OH^- from NaOH improves the catalytic efficiency of the catalyst in the hydrogen production reaction from $B_2(OH)_4$. Thus, different concentrations of NaOH were evaluated in the system (0.010 to 1.00 mol L^{-1}). It can be seen that the efficiency increases from 0 to 0.300 mol L^{-1} and decreases from 0.300 to 1.00 mol L^{-1}; therefore, the optimal concentration was 0.300 mol L^{-1}. If the concentration of OH^- is very high, the efficiency is inhibited. According to Kang *et al.*,[40] the presence of a small amount of NaOH should lead to coordination of OH^- onto the Au NPs surface, increasing its electron density. Thus, the oxidative addition of the O–H bond from water and subsequent hydrogen production are facilitated. However, excess NaOH above 0.300 mol L^{-1} apparently occupies too many surfaces Au NP sites, inhibiting substrate coordination. Therefore, the 0.300 mol L^{-1} of NaOH was maintained for further studies.

The mechanism of $B_2(OH)_4$ hydrolysis was proposed by Zhang *et al.*[13] Firstly, $B_2(OH)_4$ is adsorbed onto the catalyst surface, followed by oxidative addition of the B–B bond onto the metal surface. Two H_2O molecules act as Lewis base to coordinate two boron atoms (Lewis base). Then, the oxidative addition of an O–H bond from H_2O is facilitated by its initial coordination to the boron atoms. In sequence, occurs the formation of the two Au NPs–H bonds and the release of 2 equiv. $B(OH)_3$. Finally, the generated hydride-[M]-hydride intermediate produces H_2 upon reductive elimination.

The dose of catalyst used in the H_2 production reaction was evaluated, and the results are shown in Figure 7. Different masses of the catalyst were used, which corresponded to an Au content ranging from 0.0175 to 0.070 mmol. The best efficiency was obtained with a mass of 200 mg of catalyst (Au 0.070 mmol), i.e., 7.0 mmol%. The increase in yield can be attributed to the greater number of catalytic cycles.

The maximum hydrogen generation was calculated for the best conditions, i.e., 200 mg of catalyst containing 0.070 mmol of Au (7.0 mmol%), being 715.74 $mL_{H_2} g_{cat}^{-1} min^{-1}$ or 6.29 $mol_{H_2} mol_{cat}^{-1} min^{-1}$. Works involving the use of biochars

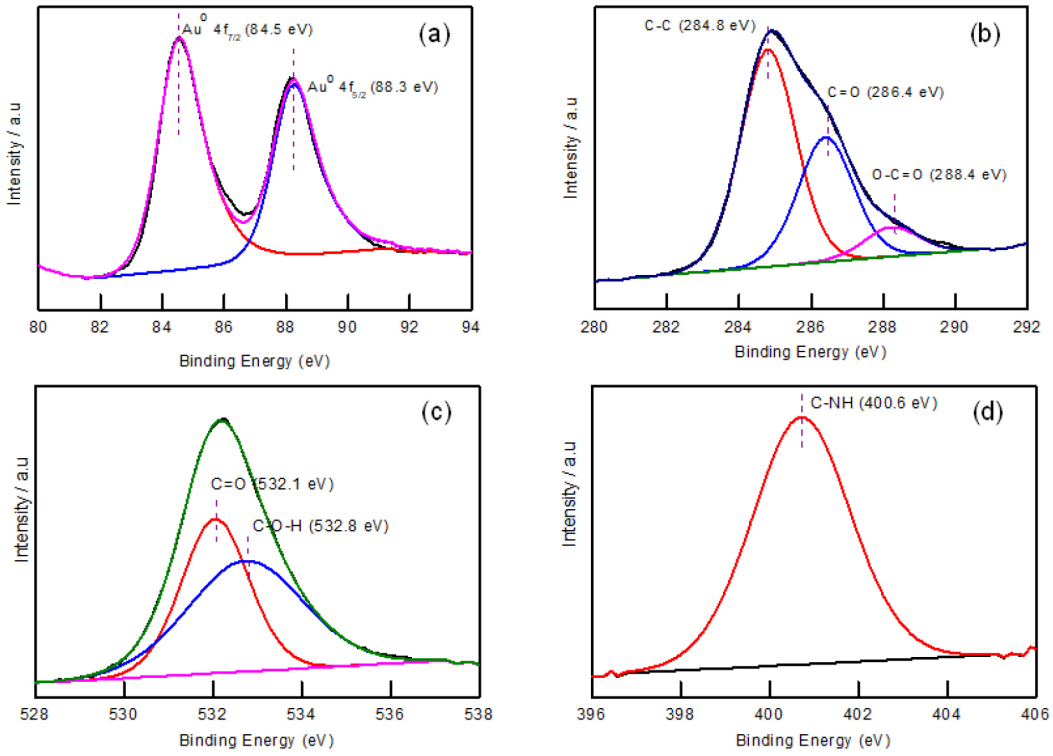

Figure 5. XPS spectra of Au-BC-triazole (a) Au 4f; (b) C 1s; (c) O 1s and (d) N 1s.

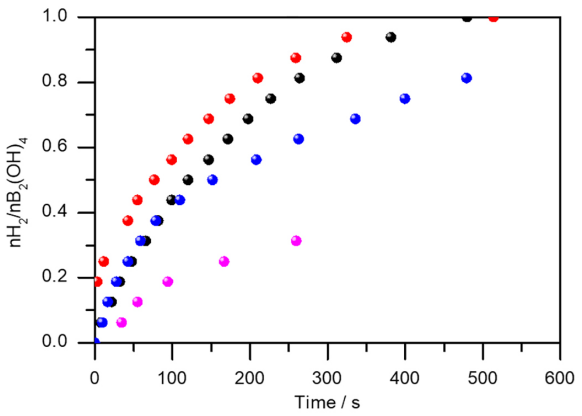

Figure 6. Evaluation of NaOH concentration in the H_2 evolution reaction. (•) 0.500 mol L^{-1}, (•) 0.300 mol L^{-1}, (•) 1.00 mol L^{-1}, (•) 0.010 mol L^{-1}. Conditions: 1.00 mmol of $B_2(OH)_4$, T = 30 °C, catalyst: 100 mg.

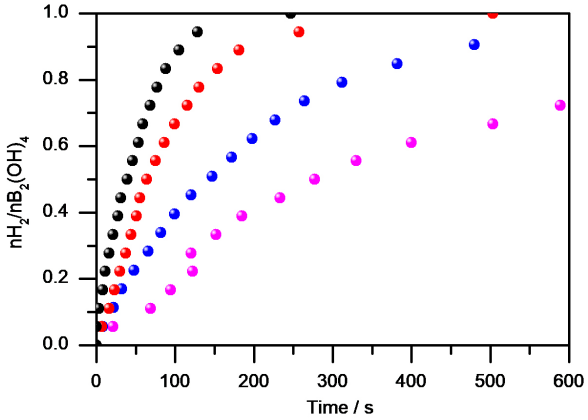

Figure 7. Evaluation of the material dose in the H_2 evolution reaction. (•) 200 mg (Au 0.070 mmol), (•) 150 mg (Au 0.0525 mmol), (•) 100 mg (Au 0.035 mmol), (•) 50 mg (Au 0.0175 mmol), conditions: 1.00 mmol of $B_2(OH)_4$, T = 30 °C, NaOH solution 0.300 mol L^{-1}.

as support in the evolution of hydrogen from hydrides are very limited. Akti[23] used pistachio shell-derived biochar supported cobalt catalysts in the H_2 evolution from $NaBH_4$. The author obtained a maximum hydrogen generation of 25 $mL_{H_2} g_{cat}^{-1} min^{-1}$. Zhou *et al.*[41] used commercial Pd/C in the hydrolysis of $B_2(OH)_4$ to produce H_2. The authors obtained 286 $mL_{H_2} g_{cat}^{-1} min^{-1}$. Therefore, it can be concluded that the results are quite promising.

Reuse assays were conducted, and the results are shown in Figure 8. It can be seen that the material is efficient until the third cycle, with a reduction in efficiency and reaction kinetics being observed in the fourth cycle. The gold nanoparticles are very stable. Thus, the recovery should be 100%.[28] The deactivation of nanomaterial can be related to its agglomeration or adsorption of product on its surface, inhibiting the access and activation of substrates to the active sites of the material.[40]

Conclusions

In this work biochar obtained from agribusiness waste (coffee straw) functionalized with triazole group was successfully used in the hydrolysis of $B_2(OH)_4$ for hydrogen

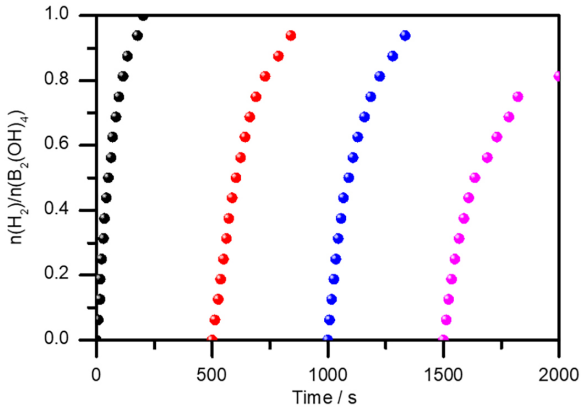

Figure 8. Reuse of the material in the H_2 evolution reaction. (•) 1st cycle, (•) 2nd cycle, (•) 3rd cycle, (•) 4th cycle. Conditions: 1.00 mmol of $B_2(OH)_4$, T = 40 °C, NaOH solution 0.300 mol L^{-1}.

generation for the first time. The functionalization of the biochar with triazole group is easily obtained through the introduction of a terminal alkyne followed by a CuAAC "click" reaction with benzylazide. The triazole formed anchored and stabilized gold nanoparticles, allowing their homogeneous distribution on the surface of biochar. In addition to avoiding agglomeration, easily visualized by microscopy images, it enabled its reuse in other catalytic cycles. The resulting material showed satisfactory reactivity in the hydrogen evolution reaction, showing the potential of this material in reactions of interest. Hydrogen produced by these processes is considered green because it does not release substances with a greenhouse effect. However, improvements to ensure its reuse in several catalytic cycles must be investigated.

Acknowledgments

CNPq (Process: 312400/2021-7), CAPES/Brazil, Process: 88881.337360/2019-01, FAPEMIG (Process: RED-00144-22), CNPq (Process: 405828/2022-5), the University of Bordeaux and the Centre National de la Recherche Scientifique (CNRS) are gratefully acknowledged.

References

1. Liu, K.-H.; Zhong, H.-X.; Li, S.-J.; Duan, Y.-X.; Shi, M.-M.; Zhang, X. -B.; Yan, J.-M.; Jiang, Q.; *Prog. Mater. Sci.* **2018**, *92*, 64. [Crossref]
2. Lalsare, A. D.; Leonard, B.; Robinson, B.; Sivri, A. C.; Vukmanovich, R.; Dumitrescu, C.; Rogers, W.; Hu, J.; *Appl. Catal., B* **2021**, *282*, 119537. [Crossref]
3. Ren, S.; Duan, X.; Ge, F.; Zhang, M.; Zheng, H.; *J. Power Sources* **2020**, *480*, 228866. [Crossref]
4. Li, Y.; Zhang, B.; Wang, W.; Shi, X.; Zhang, J.; Wang, R.; He, B.; Wang, Q.; Jiang, J.; Gong, Y.; Wang, H.; *Chem. Eng. J.***2021**, *405*, 126981. [Crossref]
5. Demirci, U. B.; *Energy Technol.* **2018**, *6*, 470. [Crossref]
6. Kang, N.; Wang, Q.; Djeda, R.; Wang, W.; Fu, F.; Moro, M. M.; Ramirez, M. D. L. A.; Moya, S.; Coy, E.; Salmon, L.; Pozzo, J.; Astruc, D.; *ACS Appl. Mater. Interfaces* **2020**, *48*, 53816. [Crossref]
7. Fu, F.; Wang, C.; Wang, Q.; Martinez-Villacorta, A. M.; Escobar, A.; Chong, H.; Wang, X.; Moya, S.; Salmon, L.; Fouquet, E.; Ruiz, J.; Astruc, D.; *J. Am. Chem. Soc.* **2018**, *140*, 10034. [Crossref]
8. Wang, Q.; Fu, F.; Yang, S.; Martinez Moro, M.; Ramirez, M. D. L. A.; Moya, S.; Salmon, L.; Ruiz, J.; Astruc, D.; *ACS Catal.* **2019**, *9*, 1110. [Crossref]
9. Michaud, P.; Astruc, D.; Ammeter, J. H.; *J. Am. Chem. Soc.* **1982**, *104*, 3755. [Crossref]
10. Jiang, S.-F.; Xi, K.-F.; Yang, J.; Jiang, H.; *Chemosphere* **2019**, *227*, 63. [Crossref]
11. Zhao, Q.; Liu, X.; Astruc, D.; *Eur. J. Inorg. Chem.* **2023**, *26*, e202300024. [Crossref]
12. Chen, W.; Shen, J.; Huang, Y.; Liu, X.; Astruc, D.; *ACS Sustainable Chem. Eng.* **2020**, *19*, 7513. [Crossref]
13. Zhao, Q.; Kang, N.; Moro, M. M.; Cal, E. G.; Moya, S.; Coy, E.; Salmon, L.; Liu, X.; Astruc, D.; *ACS Appl. Energy Mater.* **2022**, *5*, 3834. [Crossref]
14. Coşkuner Filiz, B.; Kantürk Figen, A.; Pişkin, S.; *Appl. Catal., B* **2018**, *238*, 365. [Crossref]
15. Wang, C.; Tuninetti, J.; Wang, Z.; Zhang, C.; Ciganda, R.; Salmon, L.; Moya, S.; Ruiz, J.; Astruc, D.; *J. Am. Chem. Soc.* **2017**, *139*, 11610. [Crossref]
16. Cui, C.; Liu, Y.; Mehdi, S.; Wen, H.; Zhou, B.; Li, J.; Li, B.; *Appl. Catal., B* **2020**, *265*, 118612. [Crossref]
17. Wang, C.; Ciganda, R.; Yate, L.; Tuninetti, J.; Shalabaeva, V.; Salmon, L.; Moya, S.; Ruiz, J.; Astruc, D.; *J. Mater. Chem. A* **2017**, *5*, 21947. [Crossref]
18. Pereira, R.; Astruc, D.; *Coord. Chem. Rev.* **2021**, *426*, 213585. [Crossref]
19. Daniel, M.-C.; Astruc, D.; *Chem. Rev.* **2004**, *104*, 293. [Crossref]
20. Bamdad, H.; Hawboldt, K.; Macquarrie, S.; *Energy Fuels* **2018**, *32*, 11742. [Crossref]
21. Sajjadi, B.; William, J.; Yin, W.; Mattern, D. L.; Egiebor, N. O.; Hammer, N.; Smith, C. L.; *Ultrason. Sonochem.* **2019**, *51*, 20. [Crossref]
22. Xiong, X.; Yu, I. K. M.; Chen, S. S.; Tsang, D. C. W.; Cao, L.; Song, H.; Kwon, E. E.; Ok, Y. S.; Zhang, S.; Poon, C. S.; *Catal. Today* **2018**, *314*, 52. [Crossref]
23. Akti, F.; *Int. J. Hydrogen Energy* **2022**, *47*, 35195. [Crossref]
24. Li, J.; Sun, W.; Gao, P.; An, J.; Li, X.; Sun, W.; *Sci. Total Environ.* **2021**, *761*, 144192. [Crossref]
25. Saka, C.; *Fuel* **2022**, *309*, 122183. [Crossref]
26. Saka, C.; *Appl. Catal., B* **2021**, *292*, 120165. [Crossref]

27. Saka, C.; *Int. J. Hydrogen Energy* **2021**, *46*, 26298. [Crossref]
28. Li, N.; Zhao, P.; Liu, N.; Echeverria, M.; Moya, S.; Salmon, L.; Ruiz, J.; Astruc, D.; *Chem. - Eur. J.* **2014**, *20*, 8363. [Crossref]
29. Haruta, M.; Daté, M.; *Appl. Catal., A* **2001**, *222*, 427. [Crossref]
30. Corma, A.; Garcia, H.; *Chem. Soc. Rev.* **2008**, *37*, 2096. [Crossref]
31. Alshammari, A. S.; *Catalysts* **2019**, *9*, 402. [Crossref]
32. Wang, J.; Yang, J.; Xu, P.; Liu, H.; Zhang, L.; Zhang, S.; Tian, L.; *Sens. Actuators, B* **2020**, *306*, 127590. [Crossref]
33. Sankar, M.; He, Q.; Engel, R. V; Sainna, M. A.; Logsdail, A. J.; Roldan, A.; Willock, D. J.; Agarwal, N.; Kiely, C. J.; Hutchings, G. J.; *Chem. Rev.* **2020**, *120*, 3890. [Crossref]
34. Caldera Villalobos, M.; Martins Alho, M.; García Serrano, J.; Álvarez Romero, G. A.; Herrera González, A. M.; *J. Appl. Polym. Sci.* **2019**, *136*, 47790. [Crossref]
35. Pereira, G. R.; Lopes, R. P.; Wang, W.; Guimarães, T.; Teixeira, R. R.; Astruc, D.; *Chemosphere* **2022**, *308*, 136250. [Crossref]
36. Rostovtsev, V. V.; Green, L. G.; Fokin, V. V.; Sharpless, K. B.; *Angew. Chem., Int. Ed.* **2002**, *41*, 2596. [Crossref]
37. Wang, C.; Ikhlef, D.; Kahlal, S.; Saillard, J. Y.; Astruc, D.; *Coord. Chem. Rev.* **2016**, *316*, 1. [Crossref]
38. Rasband, W. S.; *ImageJ*, version 1.51k; U. S. National Institutes of Health, Bethesda, Maryland, USA, 2017.
39. Lopes, R. P.; Guimarães, T.; Astruc, D.; *J. Braz. Chem. Soc.* **2021**, *32*, 1680. [Crossref]
40. Kang, N.; Djeda, R.; Wang, Q.; Fu, F.; Ruiz, J.; Pozzo, J. L.; Astruc, D.; *ChemCatChem* **2019**, *11*, 2341. [Crossref]
41. Zhou, J.; Huang, Y.; Shen, J.; Liu, X.; *Catal. Lett.* **2021**, *151*, 3004. [Crossref]

Submitted: May 11, 2023
Published online: July 26, 2023